**SUPPLEMENTARY INFORMATION**

## METHODS

### Purification of cell populations from peripheral blood and culture conditions

Peripheral blood (PB) samples of MPN patients and healthy donors were collected via venipuncture in EDTA-containing tubes, diluted in PBS + 2mM EDTA. Peripheral blood mononuclear cells (PBMCs) were isolated via density gradient centrifugation (Lympholyte H, Cedarlane, Burlington, Canada). CD34+ cells, CD3+ cells and CD14+ cells were positively selected from PBMCs via immunomagnetic separation, by using CD34 MicroBead Kit UltraPure, CD3 MicroBead Kit UltraPure and CD14 MicroBead Kit UltraPure respectively (Miltenyi Biotech, Auburn, CA, USA).

Granulocytes were purified from the cell pellet formed after density gradient centrifugation, containing both erythrocytes and granulocytes, by using an Ammonium chloride-based red blood cell lysis reagent.

After immunomagnetic separation, CD34+ cells were seeded at a concentration of $5 \times 10^5$ cells/ml in Iscove's modified Dulbecco's medium (IMDM) (ThermoFisher Scientific, Waltham, MA, USA) containing 20% Fetal Bovine Serum (Sigma-Aldrich, St. Louis, Missouri, United States), SCF (50 ng/ml), Flt3-ligand (Flt3L) (50 ng/ml), TPO (20 ng/ml), IL-6 (10 ng/ml) and IL-3 (10 ng/ml) (all from Miltenyi Biotech, Auburn, CA, USA).

### Next Generation Sequencing (NGS)

Targeted DNA sequencing on genomic DNA extracted from whole PB of MPN patients was performed through Capture-based target enrichment kit—CE-IVD Myeloid SolutionTM (Sophia Genetics, Lausanne, Switzerland), on the Illumina MiSeq platform. FASTQ files were processed using SOPHiA DDM platform, based

on SOPHiA Artificial Intelligence (version 4.1.1 Build 510, JSI Medical Systems, Ettenheim, Germany). The minimum required coverage was set to 1000×. The validity of the somatic mutations was checked against the publicly accessible COSMIC v69 database (http://cancer.sanger.ac.uk/cancergenome/projects/cosmic) and functional interpretation was performed using SIFT 1.03 (http://sift.jcvi.org), PolyPhen 2.0 (http://genetics.bwh.harvard.edu/pph2) and MutationTaster 1.0 algorithms (http://www.mutationtaster.org). Single nucleotide polymorphisms were annotated according to the NCBI dbSNP (http://www.ncbi.nlm.nih.gov/snp; Build 137) and gnomAD (http://gnomad.broadinstitute.org; gnomAD r2.0.1) databases.

**POU5F1 and NANOG silencing in CD34+ cells**

Frozen human CD34+ cells were transfected by using the 4D-Nucleofector System (Lonza, Basel, Switzerland). Briefly, CD34+ cells from JAK2V617F-homozygous and +9p patients were thawed and, starting from the second day after thawing, each sample was electroporated two times, once every 24 hours, with 3 µg of a small interfering RNA (siRNA) targeting human POU5F1 mRNA (ThermoFisher Scientific, siRNA ID s10873) and NANOG mRNA (ThermoFisher Scientific, siRNA ID s36650). To exclude non-specific effects caused by interfering RNA (RNAi) nucleofection, a sample transfected with a Silencer™ Select Negative Control No. 1 siRNA (ThermoFisher Scientific) was included. 12h after the last nucleofection 300 CD34+ cells from each condition were subjected to methylcellulose-based clonogenic assay.

**Quantitative real-time PCR (qRT-PCR)**

Quantitation of CD274, POU5F1 and NANOG gene expression in cDNA from Granulocytes, CD34+ cells or CD14+ cells was carried out by means of qRT-PCR. Amplification reactions were performed in triplicate for each sample, using TaqMan™ Fast Advanced Master Mix and TaqMan probes specific for CD274 (Hs00204257_m1), POU5F1 (Hs04260367_gH), NANOG (Hs02387400_g1) or GAPDH (Hs03929097_g1), used as endogenous control, on Applied BiosystemsTM QuantStudioTM 12K Flex Real-Time PCR System (ThermoFisher Scientific).
Gene expression data were analysed using the ΔΔCT method, employing healthy donors as calibrators.

**Droplet Digital PCR (ddPCR) assay**

10 ng of each DNA sample were analysed through ddPCR to quantify the JAK2p.G571S (ddPCR Mutation Assay: dHsaMDS2512546; Bio-Rad Laboratories Inc.) and JAK2V617F copies (ddPCR™ Mutation Assay: dHsaMDV27944642; Bio-Rad Laboratories Inc.). JAK2 copy number has been determined by quantifying JAK2 (using ddPCR™ Copy Number Assay: dHsaCP1000500; Bio-Rad Laboratories Inc.) and AP3B1 gene copies (ddPCR™ Copy Number Assay: dHsaCP2500348; Bio-Rad Laboratories Inc.), according to manufacturer's instructions. AP3B1 gene was employed as diploid reference for this analysis.
For coupled genomic-transcriptomic studies, isolated colonies were split in half to obtain DNA and RNA from each colony, as detailed above. JAK2V617F genotyping and JAK2 copy number analysis were performed as described above. For the quantitation of CD274, POU5F1 and NANOG gene expression, amplification reactions were performed on colonies cDNA using ddPCR Supermix for Probes (No

dUTP) (Bio-Rad Laboratories Inc.) and TaqMan probes specific for CD274 (Hs00204257_m1), POU5F1 (Hs04260367_gH), NANOG (Hs02387400_g1) or GAPDH (Hs03929097_g1), used as endogenous control (all probes from ThermoFisher Scientific).

For all ddPCR analyses, ddPCR droplets were generated on the QX200™ Droplet Generator and ddPCR reactions were performed using QX200 Droplet Digital PCR (ddPCR™) System (Bio-Rad Laboratories Inc.), setting 56°C as annealing temperature for genotyping and copy number analysis, and 59°C as annealing temperature for gene expression analysis. Positive droplets were determined using the QX200™ Droplet Reader (Bio-Rad Laboratories Inc.).

**Single cell DNA library preparation and sequencing**

Frozen PBMCs were thawed following 10× Genomics® “Sample Preparation Demonstrated Protocol” (10× Genomics, Pleasanton, CA, USA). PBMCs and CD34+ cells were mixed at a 1:1 ratio and were processed through Tapestri™ Platform (Mission Bio, San Francisco, CA, USA) as previously described(26). Barcoded samples underwent targeted PCR amplification through a custom DNA panel (Supplementary Table 2). After emulsion breaking, PCR products were purified with AMPure XP beads (Beckman Coulter, Brea, CA, USA), and Illumina i5/i7 indices were incorporated through PCR. Primer dimers were then removed through AMPure XP magnetic beads and quantified via Qubit™ 4 Fluorometer (ThermoFisher Scientific, Waltham, MA, USA) and Agilent 2100 Bioanalyzer (Agilent Technologies, Santa Clara, CA, USA). The genomic library was sequenced with 2x150bp paired-end chemistry on an Illumina NovaSeq platform (service by Macrogen Inc, Seoul, South Korea).

**Tapestri data processing**

Paired FASTQ files were analyzed through Tapestri Pipeline V2, which performs an initial quality control, adaptor trimming, reads alignment (hg19 assembly), read-cell barcode association and variant calling through GATK v.3.7 algorithm, generating a VCF file. The .h5 file created by Tapestri Pipeline was then employed for downstream analyses. Mean panel uniformity among cells was 88%. A total of 8891 cells were sequenced with 38 mean reads/cell/amplicon. Allele dropout rate was 12.75%.

Mosaic v.3.1.1 algorithm was employed to analyze clonal architecture and copy number variations (CNV). In order to get an optimal genotypization the following parameters were set: variant genotype quality > 30, at least 10 reads per cell for each variant were required to define a genotype, variants genotyped in less than 50% of cells and/or cells with less than 50% of genotyped variants were filtered out. Variants were firstly selected if detected by bulk NGS analysis. Then, germline, intronic and/or synonymous variants were filtered out. The pathogenicity of the remaining variants was then assessed by scanning Varsome database (v11.9) to retain potentially pathogenic and pathogenic variants. Next, we defined genetic clones harboring the previously identified variants. Clones were retained if present in >1% cells and harboring an allele dropout rate score <0.8.

As regards CNV analysis, amplicons were filtered in order to retain only those genotyped in >50% cells. Then, reads were normalized and the wild-type clone was set as diploid reference. To discriminate between diploid and triploid cells, the average ploidy was calculated for each amplicon. Next, 95th percentile of this distribution (2.624748) was set as threshold above which triploid cells were identified. To identify +9p cells, the mean ploidy level of the amplicons spanning

across chromosome 9p (AMP#20, #117, #118 and #119) was computed for each cell. Cells with mean ploidy > 2.624748 were referred to as +9p cells. Next, to assess the number of JAK2V617F mutated alleles in each cell, the variant allele frequency for this variant was employed to classify cells in the following categories: for diploid cells, 0%<VAF<10% defined WT cells, 10%<VAF<90% JAK2V617F heterozygous cells and VAF>90% JAK2V617F homozygous cells; for +9p cells, 0%<VAF<10% defined WT cells, 10%<VAF<50% JAK2V617F cells with 1 mutated allele, 50%<VAF<90% JAK2V617F cells with 2 mutated alleles and VAF>90% JAK2V617F homozygous cells. The distribution of cells in terms of JAK2 genotype and copy number were plotted through ggplot2 geom_jitter function.

**AKT-inhibitor treatment in CD34+ cells**

Frozen CD34+ cells from JAK2-homozygous or +9p patients were thawed and, the second day after thawing, 300 cells were seeded in triplicate in 1 ml of semisolid methylcellulose-based medium (MethoCult" GF H4434; StemCell Technologies) in the presence of 1μM MK2206 or DMSO (0.1%). Colonies were scored and individually picked after 14 days of incubation. DNA and RNA from isolated colonies underwent ddPCR as detailed below.

**Flow cytometry**

CD14+ and CD3+ cells isolated from PB of patients were incubated with “FcR Blocking Reagent, human” (Cat. no. 130-059-901) and subsequently stained using anti-PD-L1 (PE, clone 29E.2A3) and anti-CD14+ (APC-Vio770, clone TÜK4)

antibodies (1:50 in PBS 1X + 5% FBS) (all from Miltenyi Biotech) and incubate 20' at 4°C in the dark.

CD3+ cells isolated from PB of patients were stained using anti-CD3 (APC-Vio770, clone REA613) (Miltenyi Biotech), anti-CD4 (PerCP/Cy5.5, clone A161A1), anti-CD8 (FITC, clone SK1), anti-PD-1 (BV421, clone EH12.1H7), anti-PD-L1 (APC, clone 29E.2A3), anti-CD57 (Alexa Fluor 647, clone HNK-1), anti-CTLA-4 (PE/Cyanine7, clone BNI3), anti-LAG-3 (PerCP/Cy5.5, clone 11C3C65), anti-TIM3 (PerCP/Cy5.5, clone F38-2E2) and anti-CD244 (PE, clone C1.7) antibodies (1:50 in PBS 1X + 5% FBS) (BioLegend, San Diego, California) and incubate 20' at 4°C in the dark.

Cell viability of both cell populations was assessed through LIVE/DEAD™ Fixable Aqua Dead Cell Stain Kit (ThermoFisher Scientific) according to manufacturer's instructions.

**Immunofluorescence staining**

Cytospins of CD14+ cells were fixed with 4% paraformaldehyde and permeabilized using 0.2% Triton X-100 in PBS for 10 minutes. After blocking with 1% BSA in PBS, slides were incubated 16 hours at 4°C with rabbit monoclonal anti-human PD-L1 antibody (Cell Signaling Technology, Inc., Danvers, Massachusetts, USA) at 1:50 dilution. This was followed by incubation with goat anti-rabbit Alexa Fluor 568-conjugated secondary antibody (Invitrogen, Carlsbad, CA) and mouse anti-human CD14 FITC-conjugated antibody (Miltenyi Biotech), each at 1:50 dilution, for 2h at room temperature in the dark. All incubations were followed by 3 washes with PBS solution. Nuclear counterstaining was performed with 49,6-diamino-2-phenylindole (DAPI). The slides were mounted with Dako

Fluorescence Mounting Medium (Sigma-Aldrich). Finally, fluorescence imaging was performed using the Zeiss LSM 510 Meta Confocal Microscope (Zeiss, Germany) and digital images of representative areas were taken.

**Statistical analysis**

Statistical analyses were performed using GraphPad Prism version 8.4.0 (GraphPad Software, San Diego, CA, USA). After performing a normality test, comparisons between three or more groups of numerical variables with normal distribution were performed using one-way ANOVA test, while Kruskall-Wallis nonparametric test was performed for data with non-Gaussian distribution. Comparisons between two groups of numerical variables were then performed using Uncorrected Fisher's Least Significant Difference (LSD) test after one-way ANOVA test, while Uncorrected Dunn's test was performed for multiple comparisons after Kruskal-Wallis test. Two-tailed Student t-tests were employed for average comparisons in unpaired samples with Gaussian distribution, while nonparametric Mann-Whitney test was performed if samples harbored normal distribution. Categorical variables were compared through Fisher's exact test or $\chi$-square test. Sample size for each experimental condition is provided in the Figure Legends. p-values $<0.05$ were considered as statistically significant.

## FIGURE LEGENDS

**Supplementary Fig. 1: MLPA validation of Chromosome 9p amplification in patients #1-3**

**A-C** MLPA profiling of chromosome 9 copy number status in DNA extracted from Whole Peripheral Blood of Patient #1 (A), #2 (B) and #3 (C). Labels on the horizontal axis list the genomic regions detected by MLPA probes, while on the vertical axis is shown the ratio of each probe signal between the patient and the reference samples. The light blue region highlights the signal ratio of probes mapping on chromosome 9p, whereas the blue region represents the signal ratio of the probe mapping on chromosome 9q. The grey region highlights the signal ratio of reference probes. The horizontal lines represent the copy number thresholds beyond which an amplification (blue line) or a deletion (red line) are identified by Coffalyser.net software.

**A**

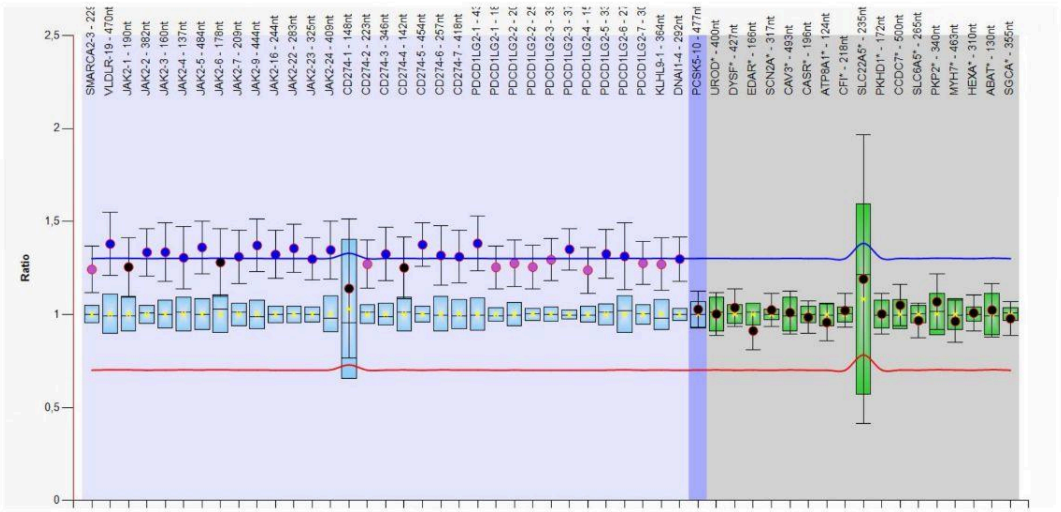
Ratio
2,5
2
1,5
1
0,5
0
SMARCA2-3 - 225
VLDLR-19 - 470nt
JAK2-1 - 190nt
JAK2-2 - 382nt
JAK2-3 - 160nt
JAK2-4 - 137nt
JAK2-5 - 484nt
JAK2-6 - 178nt
JAK2-7 - 209nt
JAK2-9 - 444nt
JAK2-16 - 244nt
JAK2-22 - 283nt
JAK2-23 - 325nt
JAK2-24 - 409nt
CD274-1 - 148nt
CD274-2 - 223nt
CD274-3 - 346nt
CD274-4 - 142nt
CD274-5 - 454nt
CD274-6 - 257nt
CD274-7 - 418nt
PDCD1LG2-1 - 43
PDCD1LG2-1 - 18
PDCD1LG2-2 - 20
PDCD1LG2-2 - 25
PDCD1LG2-3 - 39
PDCD1LG2-3 - 37
PDCD1LG2-4 - 15
PDCD1LG2-5 - 33
PDCD1LG2-6 - 27
PDCD1LG2-7 - 36
KLHL9-1 - 364nt
DNAI1-4 - 292nt
PCSK5-10 - 477nt
UROD* - 400nt
DYSF* - 427nt
EDAR* - 166nt
SCN2A* - 317nt
CAV3* - 493nt
CASR* - 196nt
ATP8A1* - 124nt
CFI* - 218nt
SLC22A5* - 235nt
PKHD1* - 172nt
CCDC7* - 500nt
SLC6A5* - 265nt
PKP2* - 340nt
MYH7* - 463nt
HEXA* - 310nt
ABAT* - 130nt
SGCA* - 355nt

**B**

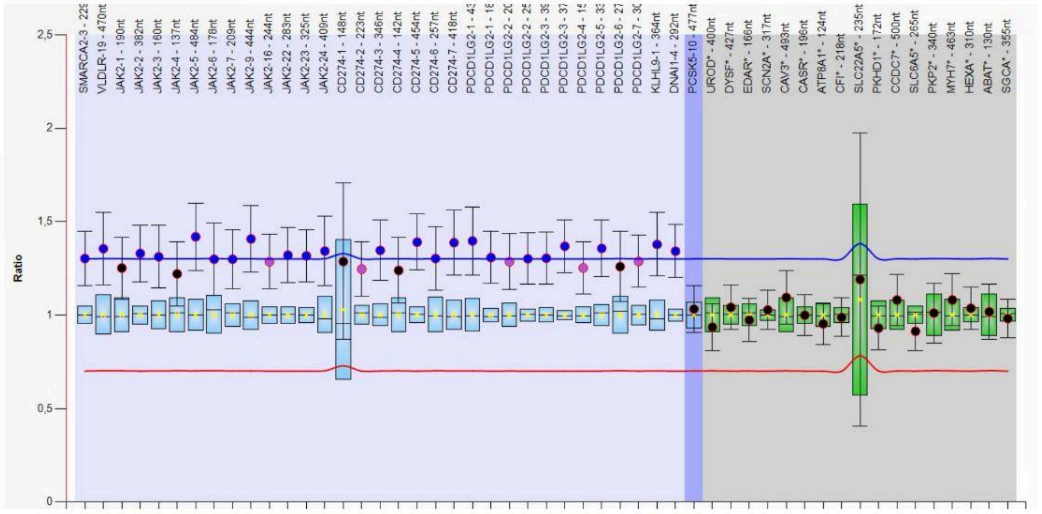
Ratio
2,5
2
1,5
1
0,5
0
SMARCA2-3 - 225
VLDLR-19 - 470nt
JAK2-1 - 190nt
JAK2-2 - 382nt
JAK2-3 - 160nt
JAK2-4 - 137nt
JAK2-5 - 484nt
JAK2-6 - 178nt
JAK2-7 - 209nt
JAK2-9 - 444nt
JAK2-16 - 244nt
JAK2-22 - 283nt
JAK2-23 - 325nt
JAK2-24 - 409nt
CD274-1 - 148nt
CD274-2 - 223nt
CD274-3 - 346nt
CD274-4 - 142nt
CD274-5 - 454nt
CD274-6 - 257nt
CD274-7 - 418nt
PDCD1LG2-1 - 43
PDCD1LG2-1 - 18
PDCD1LG2-2 - 20
PDCD1LG2-2 - 25
PDCD1LG2-3 - 39
PDCD1LG2-3 - 37
PDCD1LG2-4 - 15
PDCD1LG2-5 - 33
PDCD1LG2-6 - 27
PDCD1LG2-7 - 36
KLHL9-1 - 364nt
DNAI1-4 - 292nt
PCSK5-10 - 477nt
UROD* - 400nt
DYSF* - 427nt
EDAR* - 166nt
SCN2A* - 317nt
CAV3* - 493nt
CASR* - 196nt
ATP8A1* - 124nt
CFI* - 218nt
SLC22A5* - 235nt
PKHD1* - 172nt
CCDC7* - 500nt
SLC6A5* - 265nt
PKP2* - 340nt
MYH7* - 463nt
HEXA* - 310nt
ABAT* - 130nt
SGCA* - 355nt

**C**

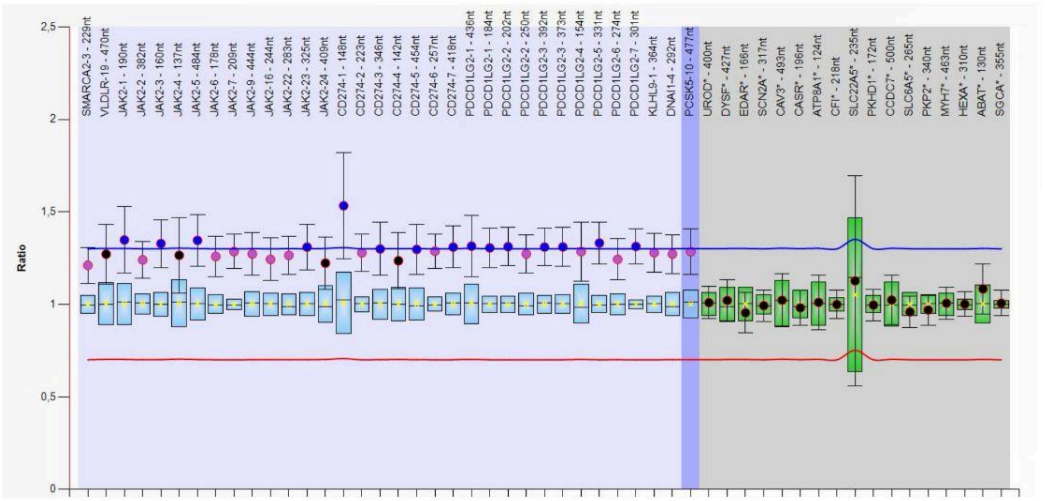
Ratio
2,5
2
1,5
1
0,5
0
SMARCA2-3 - 229nt
VLDLR-19 - 470nt
JAK2-1 - 190nt
JAK2-2 - 382nt
JAK2-3 - 160nt
JAK2-4 - 137nt
JAK2-5 - 484nt
JAK2-6 - 178nt
JAK2-7 - 209nt
JAK2-9 - 444nt
JAK2-16 - 244nt
JAK2-22 - 283nt
JAK2-23 - 325nt
JAK2-24 - 409nt
CD274-1 - 149nt
CD274-2 - 223nt
CD274-3 - 346nt
CD274-4 - 142nt
CD274-5 - 454nt
CD274-6 - 257nt
CD274-7 - 418nt
PDCD1LG2-1 - 436nt
PDCD1LG2-1 - 184nt
PDCD1LG2-2 - 202nt
PDCD1LG2-2 - 250nt
PDCD1LG2-3 - 392nt
PDCD1LG2-3 - 373nt
PDCD1LG2-4 - 154nt
PDCD1LG2-5 - 331nt
PDCD1LG2-6 - 274nt
PDCD1LG2-7 - 301nt
KLHL9-1 - 364nt
DNAI1-4 - 292nt
PCSK5-10 - 477nt
UROD* - 400nt
DYSF* - 427nt
EDAR* - 166nt
SCN2A* - 317nt
CAV3* - 493nt
CASR* - 196nt
ATP8A1* - 124nt
CFI* - 218nt
SLC22A5* - 235nt
PKHD1* - 172nt
CCDC7* - 500nt
SLC6A5* - 265nt
PKP2* - 340nt
MYH7* - 463nt
HEXA* - 310nt
ABAT* - 130nt
SGCA* - 355nt

**Supplementary Fig. 2: Association of patients' ploidy status with genetic features**

**A-B** Correlation between 9p ploidy and occurrence of High Molecular Risk (HMR) (A) or epigenetic (B) mutations. **C** Comparison of JAK2 V617F VAF between HOM and +9p patients. Results are represented as means ±SEM.

Abbreviations: 2n = diploid patients; 3n = +9p patients; HOM = JAK2-mutated homozygous patients; +9p = JAK2-mutated patients with 9p trisomy

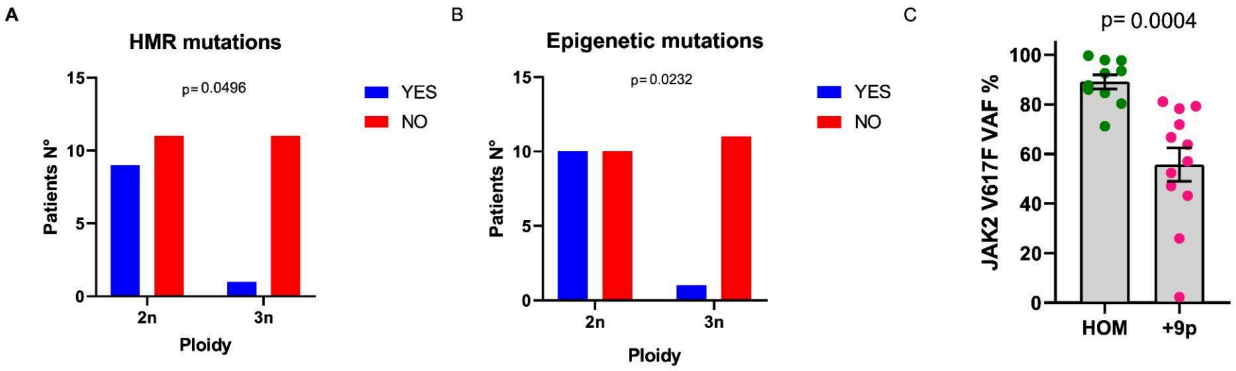

**Supplementary Fig. 3: Response to AKT inhibitor treatment in CD34+ cells from JAK2V617F-homozygous and +9p patients**

**A** Ratio between the total number of colonies grown in methylcellulose-based clonogenic assays in AKTi and UNT samples, split between HOM (n=4) and +9p patients (n=6). Results are represented as mean + SEM. **B** Ratio between the number of colonies grown in methylcellulose-based clonogenic assays in AKTi and UNT samples, split according to the different Colony-Forming Units (CFUs) in HOM and +9p patients. Results are represented as mean + SEM. **C** Barplot depicting the frequency of diploid and +9p colonies in +9p patients (n=6) in Untreated samples or after AKTi treatment.

Abbreviations: 2n = diploid colonies; 3n = +9p colonies; CFU-E/BFU-E = Colony-Forming Unit – Erythroid / Burst-Forming Unit – Erythroid; CFU-GM = Colony-Forming Unit - Granulocyte/Macrophage; CFU-G = Colony-Forming Unit – Granulocyte; CFU-M = Colony-Forming Unit – Macrophage; CFU-GEMM = Colony-Forming Unit - Granulocyte/Erythrocyte/Macrophage/Megakaryocyte; HOM = JAK2-mutated homozygous patients; +9p = JAK2-mutated patients with 9p trisomy; AKTi =AKT inhibitor, 1μM MK2206; UNT =Untreated. ** p <0.01.

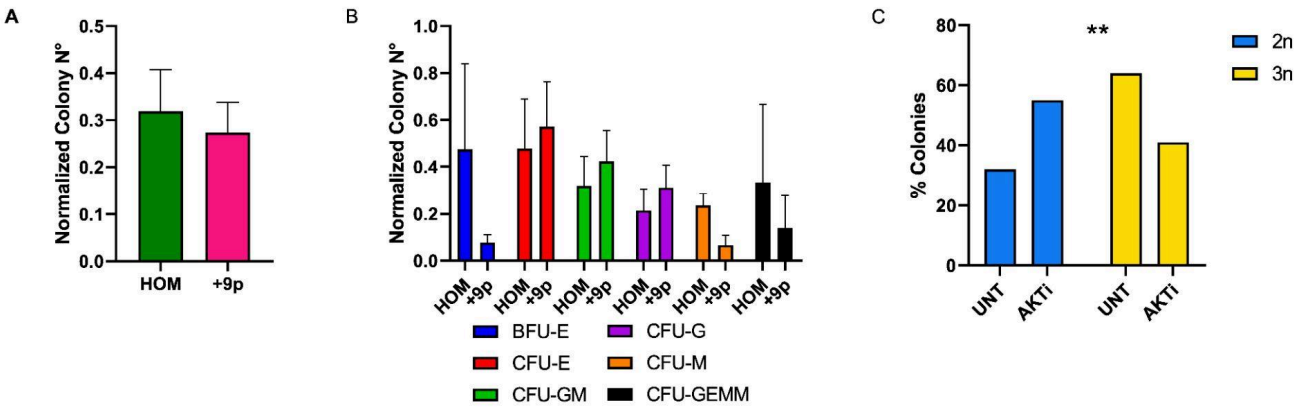

**Supplementary Fig. 4: PD-1/PD-L1 co-expression in JAK2V617F-mutated T cells**

**A** Flow-cytometric assessment of PD-1/PD-L1 co-expression in CD3+ T cells, CD4+ T-helper cells and CD8+ cytotoxic T-cells from patients (n=7 HOM, n=6 +9p) carrying JAK2V617F mutation in CD3+ cells (VAF> 5%).

Abbreviations: HOM = JAK2-mutated homozygous patients; +9p = JAK2-mutated patients with 9p trisomy

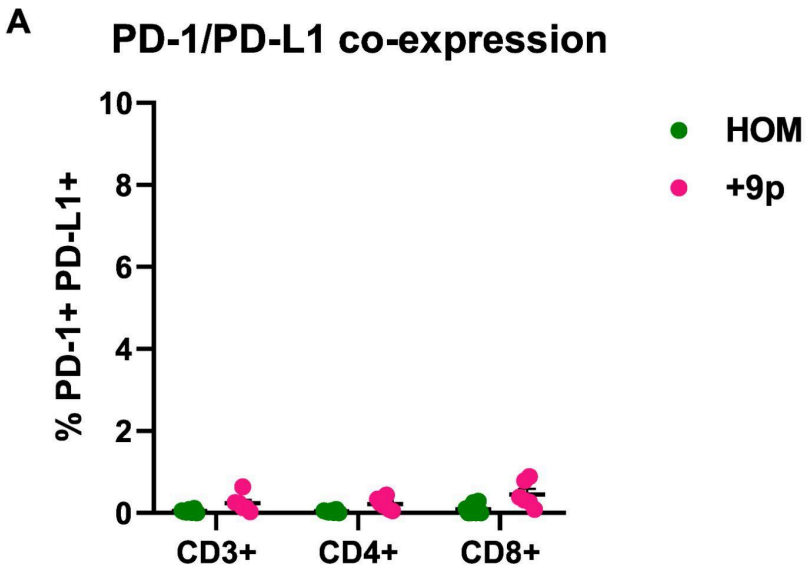

## Supplementary Table 1: Genomic features of JAK2-homozygous and +9p patients

| PATIENT | CLASSIFICATION | JAK2 V617F VAF (%) | OTHER MUTATIONS | DISEASE | KARYOTYPE |
|---|---|---|---|---|---|
| 1 | +9p | 66.7 | CSF3R p.(Met696Thr) | PMF | 46,XX,add(18)(p?13)[16]/46,XX[4] |
| 2 | +9p | 57.0 | TET2 p.(Asp1788Gly) | PMF | N/A |
| 3 | +9p | 52.4 | RUNX1 p.(Gly69Arg) | PPV | N/A |
| 4 | +9p | 47.1 | JAK2 p.(Gly571Ser) | PMF | 47,XX,+9[13]/46,XX[7] |
| 5 | +9p | 78.3 | / | PPV | 47,XY,+9[5]/46,XY[20] |
| 6 | +9p | 2.3 | / | PPV | 48,XY,+8,+9[2]/46,XY[28] |
| 7 | +9p | 79.2 | JAK2 p.(Ala654Thr), CSF3R p.(Ala119Thr) | MF | 46,XX,add(9)(p24)[8]/46,XX[15] |
| 8 | +9p | 71.9 | / | MPN-U | 49,XY,t(1;16)(q12;q11.2),+9,+9+der(16)t(1;16)(q12;q11.2)[20]/46,XY[2] |
| 9 | +9p | 25.9 | / | PET | 47,XX,+9,del(20)(q11.2q13.3)[1]/46,XX[13] |
| 10 | +9p | 63.7 | CSF3R p.(Glu405Lys) | PET | 47,XY,t(3;15)(p25;q24),+9,del(17)(q11.2q22)[22]/46,XY,t(3;15)(del(17)[3] |
| 11 | +9p | 25.9 | CEBPA p.(His195_Pro196dup), SRSF2 p.(Pro95His) | PMF | 47,XY,+9[4]/46,XY[16] |
| 12 | +9p | 81.1 | / | PMF | 47,XX,+9[2]/46,XX[22] |
| 13 | JAK2_Het | 55 | ASXL1 p.(Gly646Trpfs*12), CBL p.(Cys419Phe) | PET | 46,XX[20] |
| 14 | JAK2_Het | 43.7 | RUNX1 p.(Leu56Ser) | PMF | 46,XX,del(5)(q15q33)[20] |
| 15 | JAK2_Het | 48.4 | U2AF1 p.(Gln157Arg) | PMF | 46,XY[20] |
| 16 | JAK2_Het | 31.6 | ASXL1 p.(Pro1097Arg) | PMF | N/A |
| 17 | JAK2_Het | 54 | SRSF2 p.(Pro95His) | PMF | 46,XY[20] |
| 18 | JAK2_Het | 28.7 | ASXL1 p.(Gly646Trpfs*12), ASXL1 p.(Ser770Ter), ASXL1 p.(Glu705*), CEBPA p.(His195_Pro196dup), U2AF1 p.(Gln157Pro), EZH2 p.(Arg288Gln) | PMF | 46,XY[20] |
| 19 | JAK2_Het | 48 | / | PPV | 46,XY[20] |
| 20 | JAK2_Het | 39.7 | / | PPV | 46,XY[20] |
| 21 | JAK2_Het | 38.9 | ABL1 p.(Asn336His) | PPV | N/A |
| 22 | JAK2_Het | 22.9 | / | PMF | N/A |
| 23 | JAK2_Hom | 87.6 | CSF3R p. (Glu149Asp) | PPV | 46,XY,del(13)(q12q14),del(20)(q12)[14]/46,XY[6] |
| 24 | JAK2_Hom | 86 | ASXL1 p.(Glu635Argfs*15) | PMF | N/A |
| 25 | JAK2_Hom | 97.9 | RUNX1 p.(Arg233Profs*28), TET2 p.(Met638Ilefs*61), TET2 p.(Phe1287Leufs*76), ASXL1 p.(Met1161Thr) | PPV o PMF | 46,XX[20] |
| 26 | JAK2_Hom | 97.7 | SF3B1 p(Lys700Glu), TET2 p.(His1036Thrfs*19) | PMF | N/A |
| 27 | JAK2_Hom | 84.6 | ZRSR2 p.(Trp291*) | PPV | 46,XY[20] |
| 28 | JAK2_Hom | 80.3 | TET2 p.(Met695Cysfs*5) | PPV | N/A |
| 29 | JAK2_Hom | 99.6 | TET2 c.4044+1del | PMF | 46,XX[20] |
| 30 | JAK2_Hom | 71.2 | / | PPV | 46,XX[20] |
| 31 | JAK2_Hom | 92.5 | ZRSR2 p. (Ser447_Arg448dup), ASXL1 p.(Gly704Arg), ASXL1 p.(Ala861Thr) | PPV | 46,XX[20] |
| 32 | JAK2_Hom | 93.5 | ASXL1 p.(Ala636Val) | PET | 46,XY[20] |

**Supplementary Table 2: List of amplicons included in the single-cell genomics panel**

see attached file

**Supplementary Table 3: JAK2V617F allele frequency in cell fractions from JAK2-homozygous and +9p patients**

| PATIENT | CLASSIFICATION | JAK2 V617F VAF (%) CD34+ | JAK2 V617F VAF (%) GN | JAK2 V617F VAF (%) CD3+ | JAK2 V617F VAF (%) CD14+ |
|---|---|---|---|---|---|
| **1** | +9p | 39.6 | 65.2 | 2.2 | 64.2 |
| **2** | +9p | N/A | 57.0 | N/A | N/A |
| **3** | +9p | 56.2 | 55.1 | 0.6 | 24.3 |
| **4** | +9p | N/A | 47.1 | N/A | N/A |
| **5** | +9p | 100.0 | 91.7 | 16.1 | 86.0 |
| **6** | +9p | 41.2 | 3.9 | 10.5 | 4.6 |
| **7** | +9p | 100.0 | 66.9 | 15.8 | 80.6 |
| **8** | +9p | 84.4 | 85.8 | 26.6 | 89.3 |
| **9** | +9p | N/A | 25.9 | N/A | N/A |
| **10** | +9p | 65.5 | 63.8 | 34.2 | 69.4 |
| **11** | +9p | N/A | 25.9 | N/A | N/A |
| **12** | +9p | 100.0 | 88.1 | 8.4 | 77.2 |
| **23** | JAK2_Hom | N/A | 87.6 | N/A | 43.9 |
| **24** | JAK2_Hom | N/A | 86.0 | N/A | 90.1 |
| **25** | JAK2_Hom | N/A | 97.9 | N/A | 91.4 |
| **26** | JAK2_Hom | 92.2 | 99.0 | 3.2 | 97.8 |
| **27** | JAK2_Hom | 43.6 | 86.0 | 4.4 | 58.1 |
| **28** | JAK2_Hom | 25.0 | 88.7 | 5.6 | 61.8 |
| **29** | JAK2_Hom | 38.1 | 99.5 | 6.0 | 98.9 |
| **30** | JAK2_Hom | 21.1 | 64.6 | 2.4 | 40.5 |
| **31** | JAK2_Hom | N/A | 92.5 | N/A | 99.3 |
| **32** | JAK2_Hom | 84.5 | 97.5 | 9.4 | 96.2 |